Multimode regimes in quantum cascade lasers with optical feedback

L. L. Columbo[1,3,*] **and M. Brambilla**[2,3]

[1]*Dipartimento di Scienza e Alta Tecnologia, Università dell'Insubria, via Valleggio 11, Como, I-22100 Italy*

[2]*Dipartimento Interateneo di Fisica, Università degli Studi e Politecnico di Bari, via Amendola 173, Bari, I-70126 Italy*

[3]*Consiglio Nazionale delle Ricerche, CNR-IFN, via Amendola 173, Bari, I-70126 Italy*

[*]*lorenzo.columbo@gmail.com*

Abstract: We study the instability thresholds of the stationary emission of a quantum cascade laser with optical feedback described by the Lang Kobayashi model. We introduce an exact linear stability analysis and an approximated one for an unipolar lasers, who does not exhibit relaxation oscillations, and investigate the regimes of the emitter beyond the continuous wave instability threshold, depending on the number and density of the external cavity modes. We then show that a unipolar laser with feedback can exhibit coherent multimode oscillations that indicate spontaneous phase-locking.

OCIS codes: (140.5965) Semiconductor lasers, quantum cascade; (190.3100) Instabilities and chaos; (140.4050) Mode-locked lasers.

References and links

1. J. Faist, F. Capasso, D. L. Sivco, C. Sirtori, A. L. Hutchinson, and A. Y. Cho, "Quantum cascade laser," Science **264**, 553–556 (1994).
2. R. F. Curl, F. Capasso, C. Gmachl, A. A. Kosterev, B. Mc Manus, R. Lewicki, M. Pusharsky, G. Wysocki, and F. K. Tittel, "Quantum cascade lasers in chemical physics," Chem. Phys. Lett. **487**, 1–18 (2010).
3. J. Faist, *Quantum Cascade Lasers* (Academic, 2013).
4. A. Gordon, C. Y. Wang, L. Diehl, F. X. Kärtner, A. Belyanin, D. Bour, S. Corzine, G. Höfler, H. C. Liu, H. Schneider, T. Maier, M. Troccoli, J. Faist, and F. Capasso, "Multimode regimes in quantum cascade lasers: From coherent instabilities to spatial hole burning," Phys. Rev. A **77**, 053804 (2008).
5. C. Y. Wang, L. Kuznetsova, V. M. Gkortsas, L. Diehl, F. X. Kärtner, M. A. Belkin, A. Belyanin, X. Li, D. Ham, H Schneider, P. Grant, C. Y. Song, S. Haffouz, Z. R. Wasilewski, H. C. Liu, and F. Capasso, "Mode-locked pulses from mid-infrared quantum cascade lasers," Opt. Express **17**, 12929–12943 (2009).
6. S. Barbieri, M. Ravaro, P. Gellie, G. Santarelli, C. Manquest, C. Sirtori, S. P. Khanna, H. Linfield, and A. G. Davies, "Coherent sampling of active mode-locked terahertz quantum cascade lasers and frequency synthesis," Nat. Photonics **5**, 306–313 (2011).
7. A. K. Wójcik, P. Malara, R. Blanchard, T. S. Mansuripur, F. Capasso, and A. Belyanin, "Generation of picosecond pulses and frequency combs in actively mode locked external ring cavity quantum cascade lasers," Appl. Phys. Lett. **103**, 231102 (2013).
8. N. Yu, L. Diehl, E. Cubukcu, D. Bour, S. Corzine, G. Höfler, A. K. Wójcik, K. B. Crozier, A. Belyanin, and F. Capasso, "Coherent coupling of multiple transverse modes in quantum cascade lasers," Phys. Rev. Lett. **102**, 013901 (2009).
9. P. Dean, Y. L. Lim, A. Valavanis, R. Kliese, M. Nikolić, S. P. Khanna, M. Lachab, D. Indjin, Z. Ikonić, P. Harrison, A. D. Rakić, E. H. Linfield, and A. G. Davies, "Terahertz imaging through self-mixing in a quantum cascade laser," Opt. Lett. **36**, 2587–2589 (2011).
10. Y. L. Lim, P. Dean, M. Nikolić, R. Kliese, S. P. Khanna, M. Lachab, A. Valavanis, D. Indjin, Z. Ikonić, P. Harrison, E. Linfield, A. G. Davies, S. J. Wilson, and A. D. Rakić, "Demonstration of a self-mixing displacement sensor based on terahertz quantum cascade lasers," Appl. Phys. Lett. **99**, 081108 (2011).

#205186 - $15.00 USD Received 22 Jan 2014; accepted 17 Mar 2014; published 21 Apr 2014

11. M. C. Phillips and S. Taubman, "Intracavity sensing via compliance voltage in an external cavity quantum cascade laser," Opt. Lett. **37**, 2664–2666 (2012).
12. F. P. Mezzapesa, V. Spagnolo, A. Antonio, and G. Scamarcio, "Detection of ultrafast laser ablation using quantum cascade laser-based sensing," Appl. Phys. Lett. **101**, 171101 (2012).
13. R. Paiella, R. Martini, F. Capasso, C. Gmachl, and H. Y. Hwang, "High-frequency modulation without the relaxation oscillation resonance in quantum cascade lasers," Appl. Phys. Lett. **79**, 2526–2528 (2001).
14. D. M. Kane and K. A. Shore, *Unlocking Dynamical Diversity: Optical Feedback Effects on Semiconductor Diode Lasers* (John Wiley, 2005).
15. J. Helms and K. Petermann, "A simple analytic expression for the stable operation range of laser diodes with optical feedback," IEEE J. Quantum Electron. **26**, 833–836 (1990).
16. D. Weidmann, K. Smith, and B. Ellison, "Experimental investigation of high-frequency noise and optical feedback effects using a 9.7 μm continuous-wave distributed-feedback quantum-cascade laser," Appl. Opt. **46**, 947–953 (2007).
17. F. P. Mezzapesa, L. L. Columbo, M. Brambilla, M. Dabbicco, S. Borri, M. S. Vitiello, H. E. Beere, D. A. Ritchie, and G. Scamarcio, "Intrinsic stability of quantum cascade lasers against optical feedback," Opt. Express **21**, 13748–13757 (2013).
18. R. Lang and K. Kobayashi, "External optical feedback effects on semiconductor injection laser properties," IEEE J. Quantum Electron. **16**, 347–355 (1980).
19. T. Gensty, W. Elsäßer, and C. Mann, "Intensity noise properties of quantum cascade lasers," Opt. Express **13**, 2032–2039 (2005).
20. M. Yamanishi, T. Edamura, K. Fujita, N. Akikusa, and H. Kan, "Theory of the intrinsic linewidth of quantum cascade lasers: hidden reason for the narrow linewidth and line broadening by thermal photons," IEEE J. Quantum Electron. **44**, 12–29 (2008).
21. J. Staden, T. Gensty, W. Elsäßer, G. Giuliani, and C. Mann, "Measurements of the α factor of a distributed-feedback quantum cascade laser by an optical feedback self-mixing technique," Opt. Lett. **31**, 2574–2576 (2006).
22. R. P. Green, J. H. Xu, L. Mahler, A. Tredicucci, F. Beltram, G. Giuliani, H. E. Beere, and D. A. Ritchie, "Linewidth enhancement factor of terahertz quantum cascade lasers," Appl. Phys. Lett. **92**, 071106 (2008).
23. A. D. Rakić, T. Taimre, K. Bertling, Y. L. Lim, P. Dean, D. Indjin, Z. Ikonić, P. Harrison, A. Valavanis, S. P. Khanna, M. Lachab, S. J. Wilson, E. H. Linfield, and A. G. Davies, "Swept-frequency feedback interferometry using terahertz frequency QCLs: a method for imaging and materials analysis," Opt. Express **21**, 22194–22205 (2013).
24. F. Mezzapesa, Internal CNR-IFN report (2013).
25. A. M. Levine, G. H. M. van Tartwijk, D. Lenstra, and T. Erneux, "Diode lasers with optical feedback: Stability of the maximum gain mode," Phys. Rev. A **52**, 3436–3439 (1995).
26. T. Erneux, V. Kovanis, and A. Gavrielides, "Nonlinear dynamics of an injected quantum cascade laser," Phys. Rev. E **88**, 032907 (2013).
27. W. H. Press, B. P. Flannery, S. A. Teukolsky, and W. T. Vetterling, *Numerical Recipes in Fortran 77: The Art of Scientific Computing* (Academic, 1992).
28. L. Columbo, M. Brambilla, M. Dabbicco, and G. Scamarcio, "Self-mixing in multi-transverse mode semiconductor lasers: model and potential application to multi-parametric sensing," Opt. Express **20**, 6286–6305 (2012).

1. Introduction

Since long Quantum Cascade Lasers (QCLs) have triggered a widespread interest for several reasons: wavelength agility ($1-100THz$), high output power ($>100mW$), continuous wave (CW) emission, narrow linewidth ($<10KHz$), high speed modulation (up to several tens of GHz) [1, 2, 3]. Such features led to a row of highly prized applications in imaging, communications technology, sensing, astrophysics and space-science [3].

The search for mode-locked regimes in multimode QCLs, aiming at applications such as frequency comb generation, time-resolved measurement, and nonlinear wavelength conversion is in its initial stages. Contrary to the case of conventional bipolar semiconductor (s.c.) lasers, the fast gain recovery time of QCLs ($\sim 1ps$) due to intrasubands transitions (non-radiative phonon scattering) seems to favor the onset of multimode regimes such as those associated with the spatial hole burning and with a coherent instability similar to the Risken-Nummedal-Graham-Haken instability, although preventing spontaneous mode-locking [4]. So far, few examples of active mode-locking among longitudinal modes obtained by modulating the bias current have been recently demonstrated and used to generate ultrashort picosecond pulses [5, 6, 7]. Also, an example of stable phase coherence of multiple transverse modes is reported in [8].

#205186 - $15.00 USD Received 22 Jan 2014; accepted 17 Mar 2014; published 21 Apr 2014

From a theoretical point of view a complete understanding of the coherent multimode dynamics in QCLs is still to be achieved and this would eventually help to identify favorable phase relations for pulsed emission.

On the other side, QCLs entered with success the community of self-mixing interferometric sensing in which the laser source is used to simultaneously generate and detect electromagnetic radiation [9, 10, 11, 12]. As an emitter, a QCL is characterized by a class A dynamics, where the carriers and the polarization variables are enslaved by the electromagnetic field. This is due to high values of the ratio between photon and carrier lifetime in unipolar lasers where the latter is dominated by non-radiative phonon scattering. This unique feature leads to the absence of relaxation oscillations in the evolution of a free running QCLs towards its steady-state [13]. In the case of conventional s.c. lasers subject to optical feedback (OF) it is well known that the amplification of relaxation oscillations under increasing feedback power is the fundamental mechanism of CW destabilization, leading to chaotic dynamics [14]. Also, the linewidth enhancement factor (LEF) or Henry factor known to play a role in conventional s.c. lasers as evidenced in [15, 16], favoring stability for low values.

Recently, we predicted that a THz single mode QCL with OF, due precisely to the absence of relaxation oscillations and negligible LEF ($\alpha < 1$) can exhibit an absolute stability against OF and experiments proved that it can sustain a feedback strength ~ 70 times larger than that typically leading to the onset of chaos in a diode laser [17].

In this work we focus on the instabilities and dynamical behavior of the retroinjected QCLs, and investigate in particular the occurrence of regular oscillatory dynamics, that can be qualified as form of phase synchronization among modes. This can be an important heralding feature towards mode-locking and pulse generation. In absence of relaxation oscillations, the instability we deal with is characterized by the competition of modes, not defined by the free running laser, but by the external cavity (EC) formed by the feedback mirror and the laser output facet. As we will show, the LEF and EC length strongly influence the multimode dynamics and can either remove the instability altogether or favor a chaotic dynamics. We are of course interested in regimes comprised between the two, where regular dynamics can ensue from mode competition. To address this issue, we will adopt an essential and simple modelization of a QCL with OF, that allows us to focus on crucial dynamical parameters such as the LEF and characteristic time scales of the field and carriers dynamics. This is important to gain a physical insight towards the complex dynamics originating by the destabilization of the single mode CW emission, typical of lasers with OF [17].

The paper begins with the description and motivation of the adopted model (Sec. 2), it then proceeds with the analysis of the CW solutions and their spectral properties, with respect to the dependence on critical parameters (LEF and EC length). A Linear Stability Analysis (LSA) in Sec. 3 identifies the conditions for the loss of stability of the CW solutions and provides a simpler approximation valid for unipolar lasers. Section 4 is devoted to the analysis of the laser behavior above the instability threshold and shows the existence of regular oscillations where a number of CW solutions contributes to the emission. The conclusions are drawn in Sec. 5.

2. The model

We consider a QCL to which OF is provided by an external mirror placed at a distance L from the laser output facet as sketched in Fig. 1. The intensity of the back reflected radiation can be varied by an attenuator (not shown in the picture). We describe the system dynamics in the framework of the well known Lang-Kobayashi (LK) approach [18]. With respect to more complex descriptions of the QCL dynamical behavior based on Maxwell-Bloch equations for two [4] o three level systems [19, 20], it keeps a relatively simple formalism while still having remarkable success in describing the actual behavior of retroinjected lasers [14]. Actually it has

#205186 - $15.00 USD Received 22 Jan 2014; accepted 17 Mar 2014; published 21 Apr 2014

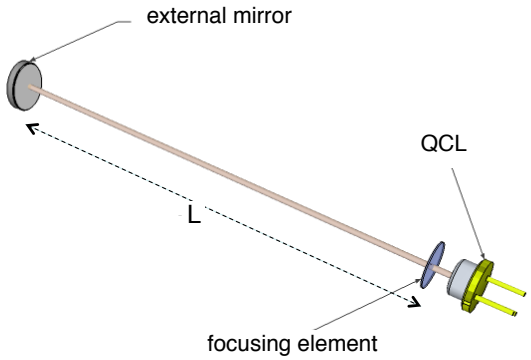

Fig. 1. Schematic layout of the self-mixing configuration. The QCL radiation is focused on the external target and re-injected into the cavity laser after a cavity round trip.

been recently used to derive relevant parameters of Mid-IR and THz quantum cascade lasers such as the LEF or to measure dynamical features of the target [21, 22, 23].

The model consists in two rate equations for the spatio-temporal evolution of the electric field and the carrier density in the laser cavity; it considers a phenomenological refractive index and gain, independent from the frequency and linearly dependent from the carriers density and a single delay term in the equation for the field. The flat gain is a sustainable approximation at this investigatory stage, since the number of external cavity modes (ECMs) we will consider and the free spectral range of the EC (EFSR) will in general allow this approximation for a QCL, whose gain width easily exceeds few THz. Another fundamental limiting assumption in the LK model is the single roundtrip approximation, where multiple reflections in the EC are neglected assuming a moderate feedback [18]. Of course, when the strength of the OF grows this approximation fails and more refined approaches must be used [14]. We nevertheless checked that even when corrections accounting for multiple reflections are introduced, the relevant dynamics remains unchanged.

The standard LK model in Eqs. (7.4) of [14] can be written in an adimensional form by introducing the field $E = \tilde{E}\sqrt{G_n \tau_e}$, the carrier density $N = (\tilde{N} - \tilde{N}_0) G_n \tau_p$:

$$\frac{dE(t)}{dt} = \frac{1}{2}(1+i\alpha)(N(t)-1)E(t) + \frac{k\tau_p}{\tau_c}E(t-\tau)e^{-i\omega_0\tau} \quad (1)$$

$$\frac{dN(t)}{dt} = \gamma\left(I_p - N(t)(1+|E(t)|^2)\right) \quad (2)$$

where G_n is the modal gain coefficient, τ_e is the carrier density decay time from the upper laser level, the time t is scaled to τ_p, the photon lifetime. The carrier density at transparency is $\tilde{N}_0$ and the pump parameter I_p is defined as $I_p = G_n \tau_p \tilde{N}_0 (G_{gen}\tau_e/\tilde{N}_0 - 1)$ where G_{gen} is electrical pumping term. Other parameters are α, the LEF; the photon to carrier lifetime ratio γ; the free running laser frequency ω_0 (equal to the laser cavity resonance) which will be the reference frequency; the laser cavity round trip time τ_c, and the EC length L which defines the delay time $\tau = 2L/c$ and of course the EFSR. The feedback parameter k depends on the effective fraction of the back-reflected field re-entering the laser ε, the laser exit facet reflectivity R and the external mirror reflectivity R_{ext} trough the relation: $k = \varepsilon\sqrt{R_{ext}/R}(1-R)$.

Looking for CW solutions of Eqs. (1) and (2) in the form $E = E_s \exp i(\omega_F - \omega_0)t$ and $N = N_s$

#205186 - $15.00 USD Received 22 Jan 2014; accepted 17 Mar 2014; published 21 Apr 2014

we get:

$$N_s = 1 - \frac{2k\tau_p}{\tau_c} cos(\omega_F \tau) \quad (3)$$

$$\omega_F = \omega_0 - \frac{k\tau_p}{\tau_c} [\alpha cos(\omega_F \tau) + sin(\omega_F \tau)] \quad (4)$$

$$|E_s|^2 = \frac{I_p}{1 - (2k\tau_p/\tau_c) cos(\omega_F \tau)} - 1 \quad (5)$$

As it is well known the s.c. laser with OF is an infinite dimensional system and its steady state characteristic might be strongly modified with respect to the free running laser case. We observe in particular that: 1) from Eq. (5) it directly follows that k is limited by $k_{max} = \tau_c/2\tau_p$; 2) Eq. (4) for the field frequency ω_F is transcendental, so its multiple solutions cannot be determined in closed form.

If not otherwise specified we use a set of parameters for the THz QCL model reported in Table 1. They refer to typical GaAs/AlGaAs heterostructures and have been derived from ex-

Table 1. *Physical parameters for a QCL in the LK model*

$R_{ext} = 0.9$	$R = 0.315$	$\omega_0 = 24.8THz$
$\gamma = 10$	$\tau_c = 37.4ps$	$\tau_p = 32.4ps$

perimental data [24, 17]. Note the large value of the photon to carrier lifetime ratio γ, a unique feature of s.c. unipolar lasers.

While the complex structure of the CW stationary solutions of this model has been studied for decades, we now dwell to some extent thereon, in order to clarify the relation among the number of solutions, their ordering with respect to the ECMs, the feedback strength and to highlighten the role of the LEF in this model.

Choosing a pump 50% above free running laser thershold ($I_p = 1.5$), $k = 0.5$, and a cavity length of $L = 146$mm (i.e. $\tau = 30$ that corresponds to a cavity round trip time of $\approx 1ns$), we report in Fig. 2(a) the complete set of CW solutions in the intensity–frequency plane ($\omega - \omega_0$, $|E|^2$) for three different values of the LEF $\alpha = 0.35, 1.3, 3$. Roughly speaking, the first two values can be considered appropriate for a THz QCL, a Mid-IR QCL [21, 22], while 3 is more typical of diode lasers. Moreover, in Fig. 2(b) we plot the frequencies of the CW solutions ω_F *vs* k for the chosen values of α. We remind that the upper limit of k in Fig. 2(b) is imposed by the self-consistency of the LK model and it is given by $k_{max} = \frac{\tau_c}{2\tau_p} = 0.58$.

Figure 2(a) shows that the CW solutions are close but not exactly coincident with the ECMs (vertical dashed lines) that are separated by the EFSR $= 2\pi/\tau \simeq 0.21$ (that corresponds to $\simeq 6.45GHz$ in physical units).

Starting from the CW closest to ω_0, the CW solutions separated by $\simeq 2\pi/\tau$ and associated with higher intensities are called "modes" of the system and correspond to in–phase interference between the electric field in the laser cavity and the reinjected delayed field. The other solutions are called "antimodes" and correspond to destructive interference; such antimodes are always unstable in standard operation as demonstrated by T. Erneux and coworkers for a diode laser [25]. Modes and antimodes appears in pairs via a saddle-node bifurcation as we increase the feedback strength.

It is important to remark that the number of CW solutions increases with increasing α. This can be understood by considering that in the hypothesis of a linear dependence of the gain G

#205186 - $15.00 USD Received 22 Jan 2014; accepted 17 Mar 2014; published 21 Apr 2014

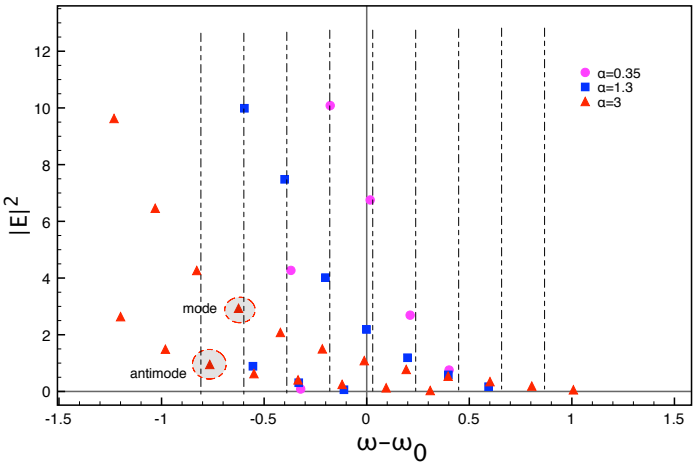

(a)

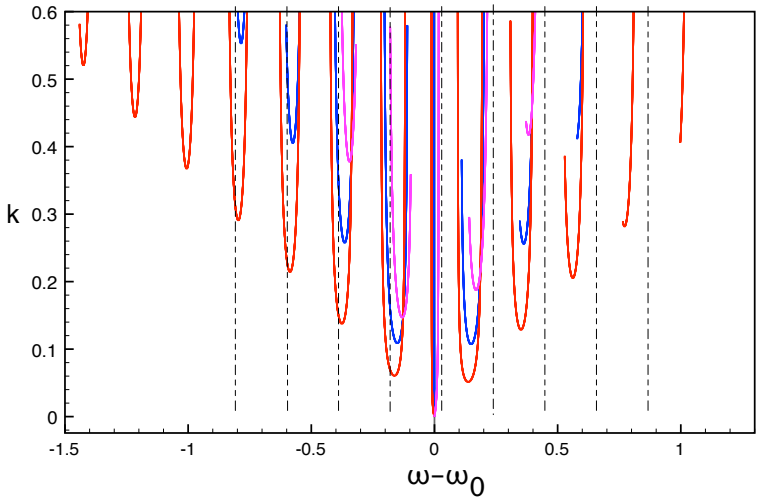

(b)

Fig. 2. (Continuous wave solutions (a) in the $(\omega-\omega_0, |E|^2)$ plane for $k=0.5$ and three values of α; (b) in the $(\omega-\omega_0, k)$ plane for three different values of α. The dashed lines represents a set of adjacent ECMs. The other parameters are: $I_p=1.5$, $\tau=30$.

and refractive index η from the carrier density N:

$$G(N)=G_{th}+\Delta N\frac{\partial G}{\partial N}\quad \eta(N)=\eta_{th}+\Delta N\frac{\partial \eta}{\partial N}$$

where G_{th} and η_{th} represent the values of G and η at threshold of the free running laser and ΔN is a small variation around the value for the carrier density at threshold, the dressed laser cavity resonances $\omega_n(N)=n\pi c/L\eta(N)$, change with N (and thus with the field amplitude E) according the formula (for a details refer to Eqs. (2.10)–(2.15) in [14]):

$$\omega_n(N)=n\pi c/L\eta(N)=\omega_0+\frac{\alpha}{2}(N-1)$$

#205186 - $15.00 USD Received 22 Jan 2014; accepted 17 Mar 2014; published 21 Apr 2014

where the phase-amplitude coupling is explicitly accounted for through the use of the $\alpha-$factor. Using Eqs. (3)–(4) the CW solutions ω_F can be expressed as:

$$\omega_F = \omega_n - \frac{k\tau_p}{\tau_c}\sin(\omega_F\tau),$$

thus in presence of feedback the CW solutions differ from the *dressed* laser cavity resonances ω_n by an amount that depends on the feedback strength. Since the EFSR is much smaller than the FSR of the laser, only the dressed cavity resonance ω_1 should be considered in the previous expression. For fixed k, an increase in α causes an increase in the separation of ω_1, and consequently of ω_F, from ω_0. In particular, the maximum distance between a CW frequency and ω_0 is given by:

$$Max(|\omega_F - \omega_0|)_k = (\alpha+1)\frac{k\tau_p}{\tau_c}. \tag{6}$$

It is thus obvious that the number of CW solutions increases with α.

We now turn our attention to the dependence of the CW solution frequencies on the feedback parameter k. A qualitative picture can be garnered from Fig. 2(b). We now fix α and, in agreement with Eq. (6), we observe that a line parallel to the $x-$axis drawn for growing values of k, will exhibit an increasing number of intersections with the e.g. red curve (α=3); this means that the number of CW solutions increases with k and their frequencies always belong to an interval centered in ω_0 with halfwidth $Max(|\omega_F - \omega_0|)_{kmax} = (\alpha/2+0.5)$. Moreover we observe that, for $k << 1$ ("bad external cavity limit") the CW solutions reduce to a single one, close the free running laser frequency ω_0, while for $k \longrightarrow k_{max}$ ("good external cavity limit") the modes approach the EC resonances i.e. the ECMs. In the following we denote as CW_0 the CW solution closest to ω_0.

The behavior of the steady state CW solutions indicates that the number of modes that can be involved in laser emission is, on the one hand, clearly linked to the EFSR, but on the other hand it can be strongly affected by the feedback strength k and by the LEF. The CW solutions stability clearly depends on such crucial parameters and a study of its boundary is presented in the next section.

3. Linear stability analysis

While the CW solutions do not depend on the field and carrier decay rates, the linear stability analysis (LSA) we will perform in this section is pivotally centered on the QCL property $\gamma >> 1$. Although we focus here on the LSA of the CW_0 solution, the same approach can be easily extended to any other CW solution.

By considering perturbations to the CW_0 solution (E_s, ω_F, N_s) in the form:

$$\delta E(t) = \delta E_s \exp(\lambda t)\exp[i(\omega_F - \omega_0)t], \quad \delta E << E_s \tag{7}$$

$$\delta N(t) = \delta N_s \exp(\lambda t), \quad \delta N << N_s \tag{8}$$

we get, after linearization, the characteristic equation for the complex eigenvalue λ

$$\lambda^3 + a_2(\lambda)\lambda^2 + a_1(\lambda)\lambda + a_0 = 0 \tag{9}$$

#205186 - $15.00 USD Received 22 Jan 2014; accepted 17 Mar 2014; published 21 Apr 2014

where:

$$a_2 = 2\frac{k\tau_p}{\tau_c}(1-e^{-\lambda\tau})\cos(\omega_F\tau)+\frac{\gamma I_p}{N_s} \quad (10)$$

$$a_1 = \left[\frac{k\tau_p}{\tau_c}(1-e^{-\lambda\tau})\right]^2+\gamma\left[2\frac{k\tau_p I_p}{N_s\tau_c}(1-e^{-\lambda\tau})\cos(\omega_F\tau)+E_s^2N_s\right] \quad (11)$$

$$a_0 = \gamma\left\{\frac{E_s^2N_sk\tau_p}{\tau_c}(1-e^{-\lambda\tau})\left[\cos(\omega_F\tau)-\alpha\sin(\omega_F\tau)\right]+\frac{I_p}{N_s}\left[\frac{k\tau_p}{\tau_c}(1-e^{-\lambda\tau})\right]^2\right\} \quad (12)$$

We observe that because of the phase invariance of Eqs. (1) and (2) we can choose E_s real without loss of generality. We define the critical feedback k_c as the minimum level causing $Max(Re(\lambda))>0$ and thus a CW instability.

At difference from T. Erneux and coworkers that in [26] are able to analytically qualify the roots of the secular equation and the associated CW instability, in the case of a single mode QCL with OF, the delay-associated nonlocality renders Eq. (9) transcendental and this prevents any analytical solution. We found the complex eigenvalues λ looking for the zeros of Eq. (9) by implementing a very precise, though CPU-intensive, minimization algorithm based on "simplex" methods [27]. We will use its results as a reference for the following approximate analysis.

In the limit $\gamma >> 1$ Eq. (9) can be reduced to the second order secular equation:

$$b_2(\lambda)\lambda^2+b_1(\lambda)\lambda+b_0=0 \quad (13)$$

where:

$$b_1 = 2\frac{k\tau_p}{\tau_c}(1-e^{-\lambda\tau})\cos(\omega_F\tau)+\frac{E_s^2N_s^2}{I_p} \quad (14)$$

$$b_0 = \frac{E_s^2N_s^2k\tau_p}{I_p\tau_c}(1-e^{-\lambda\tau})\left[\cos(\omega_F\tau)-\alpha\sin(\omega_F\tau)\right]+\left[\frac{k\tau_p}{\tau_c}(1-e^{-\lambda\tau})\right]^2 \quad (15)$$

We note that the same result, can be obtained by first adiabatically eliminating the fast variable N in the LK equations and then performing the LSA of the CW solutions of this simplified model. As we demonstrated in [17], in this case the CW instability is due to the competition among the CW solutions close to the ECMs, because the fast medium suppresses the well known mechanism of destabilization via amplification of the relaxation oscillations. In the following we now further characterize the coherent character of this instability.

The instability boundaries are found by setting $\lambda = i\Omega$, $\Omega\in\mathscr{R}$ in Eq. (13), that becomes:

$$-\Omega^2+i\Omega\left[2C(1-e^{-i\Omega\tau})\cos(\theta)+A\right]+CA(1-e^{-i\Omega\tau})\left[\cos(\theta)-\alpha\sin(\theta)\right]+C^2(1-e^{-i\Omega\tau})^2 \quad (16)$$

where to simplify the notation we introduce the quantities: $C=\tau\frac{k\tau_p}{\tau_c}$, $A=\tau\frac{E_s^2N_s^2}{I_p}$, $\theta=\omega_F\tau$
In the additional hypothesis that the instability is triggered by the competition between the stable CW and the adjacent mode and that their distance is close to $2\pi/\tau$ as discussed in the previous section, we may write:

$$\Omega\tau=2n\pi+\varepsilon;\quad 1-e^{-i\Omega\tau}\approx\frac{\varepsilon^2}{2}+i\varepsilon \quad (17)$$

where $|\varepsilon|\longrightarrow 0$ and we take $n=\pm1$.

#205186 - $15.00 USD Received 22 Jan 2014; accepted 17 Mar 2014; published 21 Apr 2014

Inserting the previous expansion in the complex Eq. (16) and neglecting terms of order $O(\varepsilon^3)$ we obtain the following system of two real second order equations for ε:

$$\varepsilon^2\left[1+2C\left(\cos(\theta)+\frac{C}{2}\right)-\frac{CA}{2}\left(\cos(\theta)-\alpha\sin(\theta)\right)\right]+4n\pi\varepsilon(1+C\cos(\theta))+4n^2\pi^2=0 \quad (18)$$

$$\varepsilon^2 4n\pi C\cos(\theta)+2\varepsilon A\left[1+C\left(\cos(\theta)-\alpha\sin(\theta)\right)\right]+4n\pi A=0 \quad (19)$$

that can be solved analytically. An instability occurs when a common solution to Eqs. (18) and (19) exists, and Fig. 3 shows the point pairs (k_c,α) that satisfy this condition and thus represent the sought CW instability boundary (dashed black line).

We compare this prediction to that obtained from the complete characteristic equation (9) (full black line) and to the instability onset obtained numerically by integrating the LK equations (open square symbols). We observe a difference of few percents or less for α values in $(1.5-2.5)$ (suitable for Mid-IR QCLs), among the complete and approximated LSA, while the numerics confirm the validity of the former one everywhere.

Finally, $\alpha_c\approx 0.35$ is the critical value of α below which no instability is found; it represents the limit of the ultra stable regime for THz QCL identified in [17].

While the decrease of the threshold with α was described for conventional inter–band lasers in [15], we stress here that the underlying physics leading to the instability is quite different.

Results from the previous section (Fig. 2), allow to better interpret Fig. 3: in particular, we ascribe the asymptotic threshold decrease to the fact that increasing α, increments the number of CW solutions existing and this favors a multimode competition. Although not reported in this paper, we extended the analysis for $\alpha>3$ and we found that the curves in Fig. 3 approach the value $k_c\simeq 0.1$, suggesting that, even in a flat gain scheme, once the number of CW solutions is large enough and their separation small enough, the destabilization takes place with a role determined (initially) by just a limited number of modes near the stable CW mode.

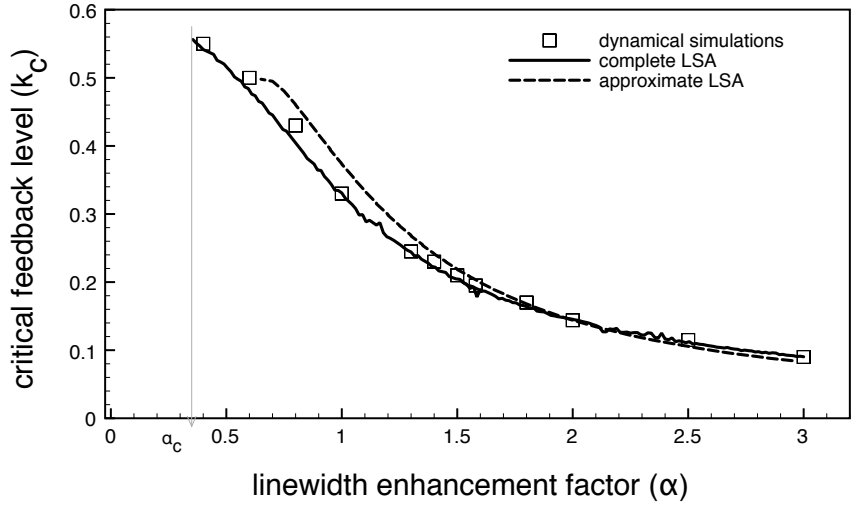

Fig. 3. Linear stability analysis of the CW solutions for $I_p=1.5$, $\tau=30$.

3.1. Variation of α_c with τ

Since an increasing EC round trip time τ implies more and denser CW solutions (see Eq. 4), we study the variation of the CW instability boundaries, and in particular of α_c, with this

#205186 - $15.00 USD Received 22 Jan 2014; accepted 17 Mar 2014; published 21 Apr 2014

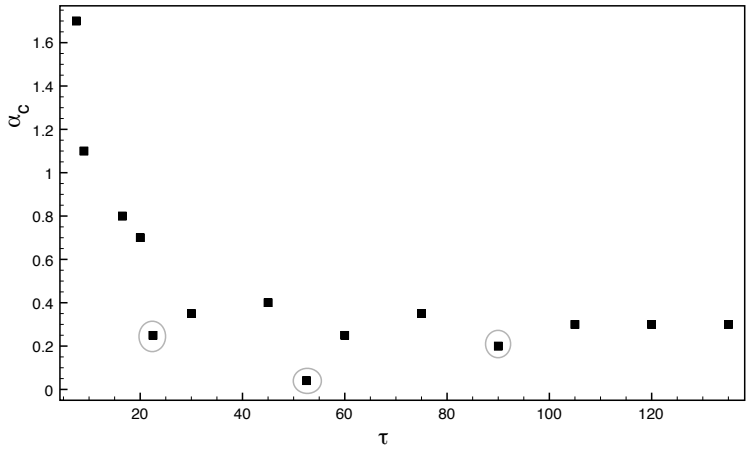

Fig. 4. $I_p = 1.5$. Numerically calculated values of α_c against τ.

parameter. In Fig. 4 we plot the numerically calculated values of α_c versus τ for $I_p = 1.5$. As expected from the considerations reported in previous section, we observe that a smaller τ (i.e. less solutions and more spaced ECMs) causes the onset of a CW instability for larger values of α (up to $\alpha_c = 1.7$ for $\tau = 7.5$). Moreover when τ becomes larger than $\simeq 80$, the ECMs are so close that the number of competing CW modes leading to the CW instabilty does not really depend on α, so that α_c shows a general asymptotic behaviour towards $\alpha_c \simeq 0.3$. The THz QCLs ultrastability is thus confirmed over a very large range of τ, or equivalently of EC lengths.

In Fig. 4 though, some values of τ (evidenced by circles) can be noted, where the threshold drops (i.e. the system is more prone to destabilize the stationary emission). By analyzing the values $\tau = 22.5$, 52.5 and 90, we noted that the frequency of the free running laser frequency ω_0 there falls close (less than $1/3$ of the EFSR) to midway between two adjacent ECMs. This is a situation where the competition between the modes is strongest and thus leads to easier destabilization. In fact, by studying the distance of the closest (to the emitted one) CW mode from the neighboring ECMs, one sees that it diminishes with increasing k, keeping always smaller than for neighboring values of τ. This also tells us that the instability of this system is a complex mechanism where the number of solutions and the EFSR isn't the only criterion involved, but the relative positions of the frequencies of the free-running laser, CW solutions and ECMs play a role.

4. Dynamical simulations

In this section we study the dynamical behavior of the laser when the instability, studied in the previous section, occurs and the steady states the laser achieves thereupon. Equations (1) and (2) were integrated with a $6th$ order Adams-Bashforth-Moulton predictor-corrector algorithm with fixed pump I_p and EC length L (or, equivalently, the delay τ).

We studied the dynamical regimes when the feedback k is increased across the threshold k_c for different values of α.

As a general rule, we identify different dynamical regimes.

- For values of α close to zero ($\alpha \leq \alpha_c$), typical of THz QCLs, the LSA does not predict an instability boundary for $k < k_{max}$, the laser never destabilizes the continuous wave solu-

#205186 - $15.00 USD Received 22 Jan 2014; accepted 17 Mar 2014; published 21 Apr 2014

tion closest to the free running laser frequency ω_0 denoted here as CW_0. This corresponds to the ultrastable regime reported in [17]

- For values of α larger than α_c, but still smaller than a second critical value that we denoted as α_{sw}, the CW_0 destabilization leads the laser to switch to an adjacent CW mode, and the emission is still constant (see subsection 4.1 for details)

- For $\alpha > \alpha_{sw}$ we observe a Hopf bifurcation leading to the onset of a regime of regular oscillations given by the locking among few (usually two) CW modes as soon as the feedback strength k overcomes k_c. A further increase of k leads to the destabilization of this regular regime to a stronger multimode competition that is generally associated with a chaotic dynamics. For even higher feedback the system shows one of the following dynamical behaviors: 1. a single chaos crisis leading to the restoration of single mode operation on a different CW mode with constant intensity; 2. windows of chaotic behavior alternated with single CW operation or regular oscillations; 3. a chaotic system dynamics (see subsection 4.2).

As an illustrative case, in the next two paragraphs we describe the system dynamical behavior beyond the CW instability threshold for $I_p = 1.5$, and $\tau = 30$ (for which $\alpha_c = 0.35$).

4.1. CW-solution switching and multimode regimes of stationary emission

In Fig. 5 we plot for $\alpha = \alpha_{sw} = 1.3$ the maximum and minimum values of the intensity $I = |E|^2$ during a ramp in k from 0 to 0.5. To avoid transient latency, the system was allowed to relax to steady state before changing k by each step.

On the overall, in all cases where $\alpha_c \leq \alpha \leq 1.3$, all instabilities met by increasing k cause the switching of a stationary emission from a CW mode (for $k << 1$ the laser starts from CW_0) to the adjacent one. This corresponds to the system transitions from region *I* to region *II* and from region *II* to region *III* in Fig. 5. The switches are accompanied by a transient oscillation that can be seen in Fig. 5 immediately after the thresholds.

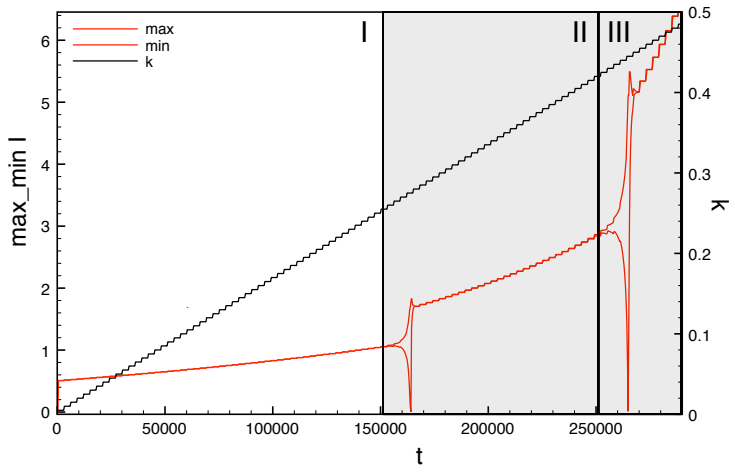

Fig. 5. $I_p = 1.5$, $\tau = 30$, $\alpha = 1.3$. Maximum and minimum value of the intensity obtained by gradually increasing k during the system dynamical evolution. The corresponding values of k are reported on the right vertical axis.

#205186 - $15.00 USD Received 22 Jan 2014; accepted 17 Mar 2014; published 21 Apr 2014

4.2. *Multimode regimes: irregular dynamics and locked states of regular high contrast oscillations*

When we depart from the regime of CW-switching, e.g. by increasing α, we observe a dynamics where a limited number of modes appear in the optical spectrum. The regular oscillations appearing in the intensity proves that the modes have a constant phase relation. As an example Fig. 6(a) shows the system bifurcation diagram obtained as described in the previous paragraph for $\alpha = 3$. While in region *I*, the solution CW_0 is stable, in the grey areas (regions *II*, *III*, *IV*, *V*) the CW emission is unstable showing regular oscillations or a chaotic dynamics. In Fig. 6(b) we show the power spectra for fixed values of k in the CW unstable regimes as marked by the corresponding roman numbers.

In particular we observe that when $k > k_c$ the system enters a regime of regular oscillations (see region *II* in Fig. 6(a) and in Fig. 6(b). An inspection of the spectrum (see Fig. 6(c) for $k = 0.12$), reveals a main peak at the frequency difference between the CW_0 and the next stationary solution denoted as CW_1. The period of these oscillations varies with k and α according to the dependency of the CW modes on k as illustrated in Fig. 2(b) and thus can be somewhat different from the cavity round trip time τ. For the parameters in Fig. 6 the period of the oscillations is $\Delta t \sim 1.2\tau = 35$. By further increasing k the system enters a chaotic regime characterized by continuous and multipeaked spectra with still dominant contributions linked to the CW modes (see regions *III* and *V* in Figs. 6(a) and 6(b)). An example of this irregular dynamics is shown in the spectrum and intensity plot in Fig. 6(d) for $k = 0.163$ where the ECMs are indicated by vertical dashed lines. Interspersed within the chaos region, one meets windows of regular oscillations (see region *IV* in Figs. 6(a) and 6(b) where again the multimode coherent competition shows a regular dynamics with a period slightly variable with k. This is known to occur also in bipolar lasers with phase–conjugated feedback (see chap.2 of [14]), where windows of periodic orbits are separated from each other by "bubbles" of irregular dynamics, and the onset of chaos is associated with a torus breakup.

A detailed behavior of the oscillations in the regular regimes is shown in Fig. 6(f) where we plot the correlation diagram for three different values of k belonging to the regions *II*, *III* and *IV*. The intensity $I(t+\Delta t)$ is plotted against $I(t)$ with $\Delta t = 1.2\tau$. The points corresponding to regular intensity oscillations in region *II* and *IV* depict two distinct limit cycles corresponding to slightly different periods, while those corresponding to the irregular oscillations of region *III* are more scattered but their density is higher around the two limit cycles, since the dominant contribution in system dynamics is linked to the CW modes.

The stable periodic oscillations in Fig. 6(e) for $k = 0.2$ represent the phenomenon of coherent dynamics involving the largest number of modes ($\simeq 5$ in the first decade of the power spectrum) that we were able to simulate for the chosen values of I_p and τ and we believe that it can be considered an interesting phenomenon of coherent synchronization of multimode emission. Here, without external modulation of laser gain (as in active mode-locking [5, 6]), the system shows a self-organization of its emission with a (still limited) comb of ECMs. This is a condition that may hint towards a spontaneous mode-locking in a QCL with feedback.

Since we are interested in QCLs, we scanned smaller values of α. Of course the reduction in the number of solutions this implies, must be compensated by an increase of the EC length (i.e. of τ) in order to have a sizable number of modes to compete and possibly lock in phase. We found that the regime of coherent phase synchronization is rather widespread and it even occurs close to the first instability window. We report here on $\alpha = 2$, a value that is still compatible with experimental evidences (a value as high as 2.5 is reported in [21]) and shows phase coherence to appear for still moderate EC lengths.

As shown in Fig. 7 for $\tau = 60$ and $k = 0.13$, close to the instability threshold of the CW_0 solution and before any chaotic crisis, a regime of nontrivial regular oscillations appears where

#205186 - $15.00 USD Received 22 Jan 2014; accepted 17 Mar 2014; published 21 Apr 2014

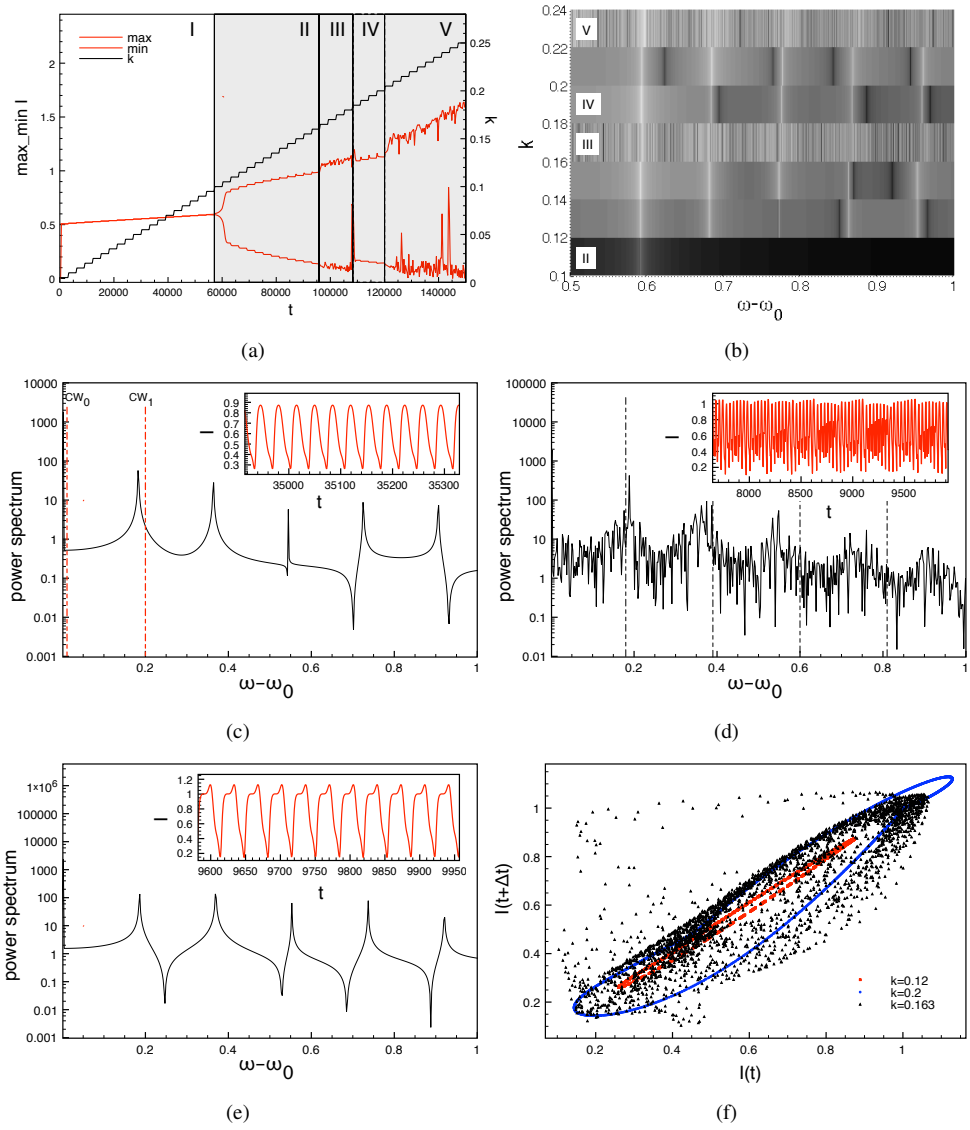

Fig. 6. $I_p = 1.5$, $\tau = 30$, $\alpha = 3$. (a), (b) Maximum and minimum value of the intensity and intensity power spectrum obtained by gradually increasing k during the system dynamical evolution. (c)-(e) Power spectrum and temporal variation of the intensity for $k = 0.12$ (c), $k = 0.163$ (d) and $k = 0.2$ (e). (f) Correlation plot for $\Delta t = 1.2\tau = 35$ and three different values of k.

the $\simeq 5$ CW modes are present in the first decade. For $k > 0.2$ a complex multimode competition causes the first abrupt transition to a highly irregular regime.

As anticipated, we verified that the regimes of coherent phase synchronization we met in different parametric conditions, are sustained even when multiple reflections in the EC are taken into account. While the model extension is outside the scope of this paper, we relied on previous knowledge gathered in [28] and adopted an expression of the feedback field generalized to an arbitrary number of reflections (see Eqs. (15) and (17) in [28]). The general indications of the

#205186 - $15.00 USD Received 22 Jan 2014; accepted 17 Mar 2014; published 21 Apr 2014

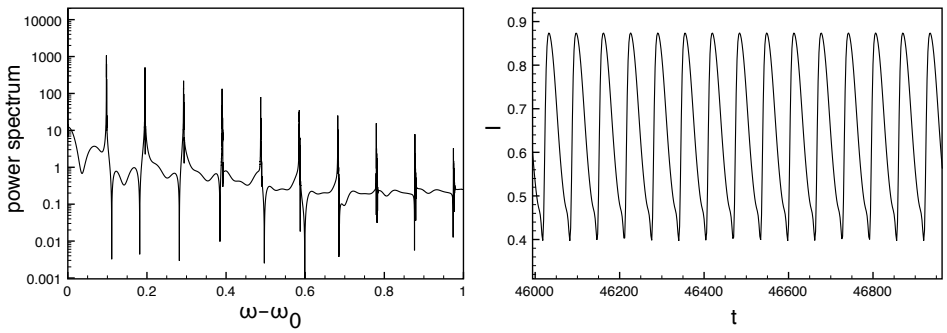

(a) (b)

Fig. 7. $I_p = 1.5$, $\tau = 60$, $\alpha = 2$. Power spectrum (a) and temporal variation (b) of the field intensity showing a regime regular multimode dynamics for $k = 0.13$.

extended model is that, of course, instability threshold values for k may vary, but the dynamical scenery remains qualitatively the same: at threshold one meets the onset of laser regular oscillations, linked to the competition of two adjacent ECMs, which upon increasing k show first the occurrence of more modes, locked in phase and still producing a regular intensity pulsation, and then the system abruptly plunges into a chaotic behavior, which again is interrupted by windows of regular dynamics.

5. Conclusions

In conclusion, we analyzed the stationary solutions of a QCL with optical feedback and showed their dependencies on critical parameters such as the LEF and the EC length, we provided an exact LSA and a simpler, approximated one, valid for unipolar lasers which allows to study the destabilization of the CW_0 mode and also validates and extends the prediction of a regime of absolute stability of THz QCLs against OF. By studying the behavior of the laser above the instability threshold we could evidence the multimode dynamics typical of unipolar lasers where the mechanism of amplification of relaxation oscillations is absent and the emission is determined by the competition of several modes; in particular at threshold or in the windows of regular dynamics between chaotic islands, we could prove the existences of regimes of coherent multimode oscillations emerging from very simple physical processes in a 2-level model with feedback, which could possibly indicate a path towards spontaneous mode-locking.

Acknowledgments

This research has been funded by the Italian Ministry of Research (MIUR) through the Futuro in Ricerca FIRB-grant PHOCOS (RBFR08E7VA). The authors also acknowledge support from MIURPON02-0576 INNOVHEAD and MASSIME.